Available online at www.sciencedirect.com
SCIENCE DIRECT®
PERGAMON
Applied Geochemistry 19 (2004) 55–72
Applied Geochemistry
www.elsevier.com/locate/apgeochem

Organic geochemistry across the Permian–Triassic transition at the Idrijca Valley, Western Slovenia

Valérie Schwab, Jorge E. Spangenberg*

Institut de Minéralogie et Géochimie, Université de Lausanne, BFSH-2, CH-1015 Lausanne, Switzerland

Received 29 April 2002; accepted 10 June 2003
Editorial handling by B.R.T. Simoneit.

Abstract

Bulk and molecular stable C isotopic compositions and biomarker distributions provide evidence for a diverse community of algal and bacterial organisms in the sedimentary organic matter of a carbonate section throughout the Permian–Triassic (P/Tr) transition at the Idrijca Valley, Western Slovenia. The input of algae and bacteria in all the Upper Permian and Lower Scythian samples is represented by the predominance of C_{15}–C_{22} *n*-alkanes, odd C-number alkylcyclohexanes, C_{27} steranes and substantial contents of C_{21}–C_{30} acyclic isoprenoids. The occurrence of odd long-chain *n*-alkanes (C_{22}–C_{30}) and C_{29} steranes in all the samples indicate a contribution of continental material. The decrease of C_{org} and C_{carb} contents, increase of Rock-Eval oxygen indices, and ^{13}C-enrichment of the kerogen suggest a decrease in anoxia of the uppermost Permian bottom water. The predominance of odd C-number alkylcycloalkanes, C_{27} steranes, and C_{17} *n*-alkanes with $\delta^{13}C$ values $\sim -30‰$, and ^{13}C-enrichment of the kerogens in the lowermost Scythian samples are evidence of greater algal productivity. This increased productivity was probably sustained by a high nutrient availability and changes of dissolved CO_2 speciation associated to the earliest Triassic transgression. A decrease of C_{org} content in the uppermost Scythian samples, associated to a ^{13}C-depletetion in the carbonates (up to 4‰) and individual *n*-alkanes (up to 3.4‰) compared to the Upper Permian samples, indicate lowering of the primary productivity (algae, cyanobacteria) and/or higher degradation of the organic matter.

1. Introduction

The Permian–Triassic (P/Tr) boundary, 251.4±0.3 Ma ago, is marked by the most drastic mass extinction in the Phanerozoic fossil record, with more than 90% of marine species, 60% of reptile and amphibian families, 30% of insect species, 70% of terrestrial vertebrate genera, and most land plants dying out (Raup, 1979; Erwin, 1994; Stanley and Yang, 1994). Many hypotheses have been proposed to explain this biological crisis, including bolide (asteroid or comet) impact (Rampino and Haggerty, 1996), massive flood basalt and pyroclastic volcanism (Campbell et al., 1992; Renne et al., 1995; Bowring et al., 1998), environmental changes (Thackeray et al., 1990; Stanley and Yang, 1994; Retallack, 1999), or ocean anoxia (Wignall and Hallam, 1992; Knoll et al., 1996; Wignall and Twitchett, 1996; Hotinski et al., 2001). However, most of the hypotheses proposed as cause for the P/Tr mass extinction do not account for all observed taxonomic, physiological, ecological, and biogeographic patterns of extinction, and do not provide geological and geochemical tests of proposed causal mechanisms (e.g., Erwin, 1994). Therefore, Erwin (1996) proposed a synergistic combination of these events as the most plausible cause of the P/Tr mass extinction. Recent statistical analysis of species stratigraphy ranges (Jin et al., 2000), high-resolution cyclostratigraphy (Rampino et al., 2000) and U/Pb zircon

* Corresponding author. Tel.: +41-21-692-4365; fax: +41-21-692-4305.
E-mail address: jorge.spangenberg@img.unil.ch (J.E. Spangenberg).

0883-2927/$ - see front matter © 2003 Elsevier Ltd. All rights reserved.
doi:10.1016/S0883-2927(03)00127-6

geochronology (Bowring et al., 1998) studies have proven the rapidity (< 500 to ~8 ka) of the P/Tr extinction, supporting the hypothesis of a catastrophic (bolide, volcanism) cause of the mass extinction. Becker et al. (2001) reported extraterrestrial isotopic signature of He and Ar encapsulated in fullerenes in sediments from 3 P/Tr boundary localities in different continents, thus providing evidence that an extraterrestrial impact event accompanied the mass extinction.

Stable isotopic composition of organic matter and carbonates are widely used as an indicator of depositional environment, and for the assessment of paleoclimates and paleoceanography of ancient marine environments (e.g., Schidlowski, 1982; Anderson and Arthur, 1983; Veizer, 1983). However, interpretations of these isotopic records are often complicated by (inorganic and organic) chemical and isotopic exchanges, variations in Eh, pH, salinity, temperature, CO_2 partial pressure (pCO_2), and bacterial activity during post-depositional diagenetic/metamorphic fluid–fluid and fluid–rock mixing processes (e.g., Galimov, 1985). Combined organic geochemical and isotopic studies may help to overcome these difficulties. The distributions of hydrocarbons from ancient sediments have been used to infer biological origin, maturity, and proportions of marine and terrestrial organic matter, as well as sedimentary facies and paleosalinity (Meinschein, 1969; Tissot and Welte, 1984; Grimalt and Albaigés, 1987). The C isotopic composition of bulk organic matter (kerogen) helps to distinguish the different (terrigenous, marine) organic sources (Schidlowski, 1982). The isotopic compositions of the individual hydrocarbons serve to identify the biological precursors of hydrocarbons in ancient sediments (e.g., Freeman et al., 1990).

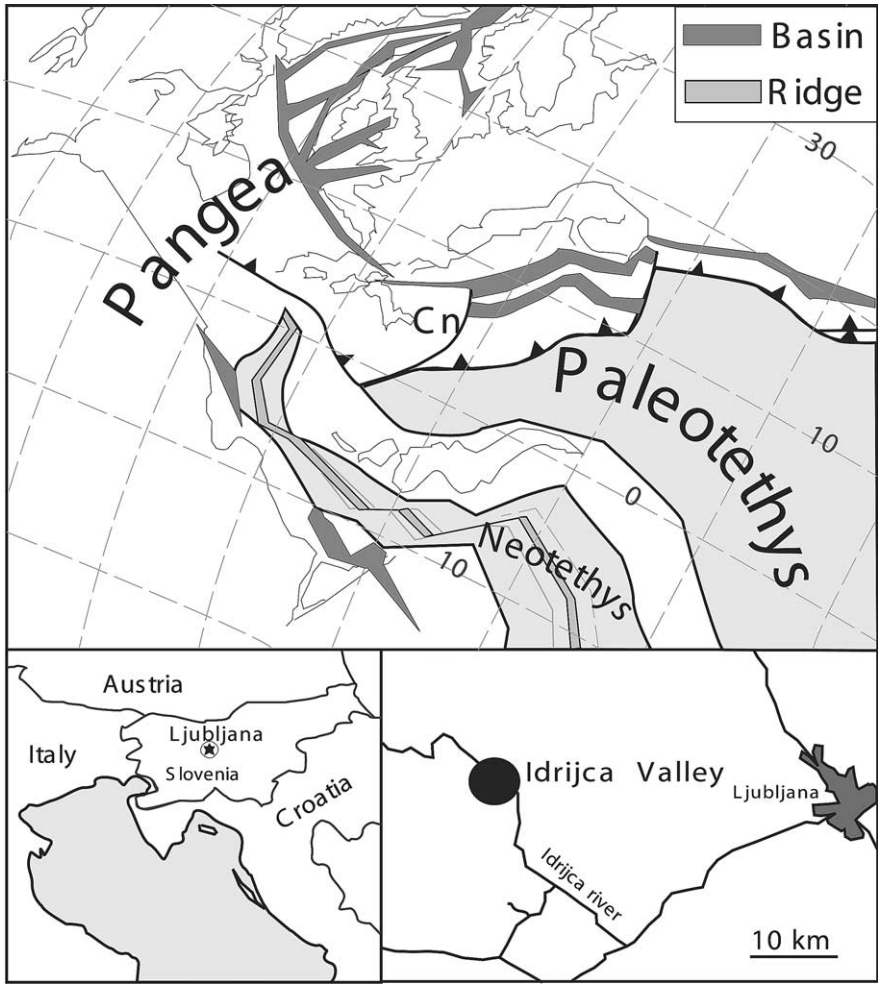

Fig. 1. Paleogeographic reconstruction for the latest Permian after Stampfli et al. (2001) showing the location of the Carnic Alps (Cn) area. Inserts give the location of the P/Tr section at the Idrijca Valley, Slovenia.

This paper presents organic geochemical and isotopic data for the nonmetamorphosed carbonate rocks of the Permian–Triassic section at the Idrijca Valley in Western Slovenia (Fig. 1). For this P/Tr section, sedimentological and palynological studies (Ramovš, 1986; Dolenec et al., 1999) as well as stable C isotope measurements of carbonates and total organic matter (Baud et al., 1989; Dolenec et al., 2001), magnetostratigraphic and major and trace elements data (Dolenec et al., 2001) have been published. Baud et al. (1989) reported the first C isotope profile of Upper Permian to Lower Triassic strata of the Idrijca Valley section, and compared it with other Tethyan sections in the Southern Alps. Recently, Dolenec et al. (2001) documented that the disappearance of typically Upper Permian fauna at the P/Tr boundary at Idrijca is accompanied by a negative isotopic shift of the inorganic ($\delta^{13}C_{carb}$) and total organic ($\delta^{13}C_{org}$) C, an enrichment in most major and trace elements and a sharp magnetic susceptibility pulse. The presence of a sharp negative $\delta^{13}C_{org}$ shift at the P/Tr boundary, followed by an abrupt positive shift 6 cm above the boundary, suggests an interruption of the long-term gradual processes recorded by the $\delta^{13}C_{carb}$ curve (Dolenec et al., 2001).

The aim of this study was to define better the type and magnitude of the biogeochemical changes during the mass extinction in this region of the southern Alps. New results are presented from Rock-Eval pyrolysis, kerogens ($\delta^{13}C_{ker}$), and soluble organic matter ($\delta^{13}C_{EOM}$), biomarker distributions, and $\delta^{13}C$ of individual alkanes.

2. Geologic setting

The Permian–Triassic section at the Idrijca Valley is situated in the Carnic Alps, 20 km west of Ljubljana, western Slovenia (Fig. 1). The section is composed of one of the more marine Permian–Triassic rocks in the Alpine area (Baud et al., 1989). Paleogeographic reconstructions place these sediments in a fore-arc basin setting in the northeastern Paleotethys (Fig. 1). Sedimentologic and preliminary paleontologic studies are given in Ramovš (1986) and Dolenec et al. (2001). The Upper Permian at Idrijca Valley represents the uppermost 250 m-thick Žažar Formation, which consists of black, well bedded, and abundantly fossiliferous shallow marine carbonates (Fig. 2). The upper part of the Formation (Dorashamian) is composed of 5–40 cm thick dark grey and black limestone layers interbedded with rare black shale. Limestone microfacies are represented mostly by packstones and grainstones, partly wackestones very rich in microfossils, composed mainly by calcareous algae and foraminiferae (Ramovš, 1986). The topmost part of this unit is characterized by a 20 cm thick black algal packstone, containing fragments of calcareous algae and foraminiferae, and echinoderms (Dolenec et al., 2001). The faunal composition displays gradual impoverishment of Upper Permian taxa moving upward towards the boundary and an abrupt disappearance at the boundary. The P/Tr boundary is sharp, not erosional and is marked by an up to 0.8 cm thick clayey marl layer. The deposition of the P/Tr boundary layer most probably took place during a period of maximum eustatic sea level fall (Dolenec et al., 1999). The boundary layer is followed by a light grey well bedded Lower Scythian sparitic dedolomitized limestone of Griesbachian age. Upward, laminated dolomitic limestone alternating with grey stylolithic dolomites follows the sparitic limestone.

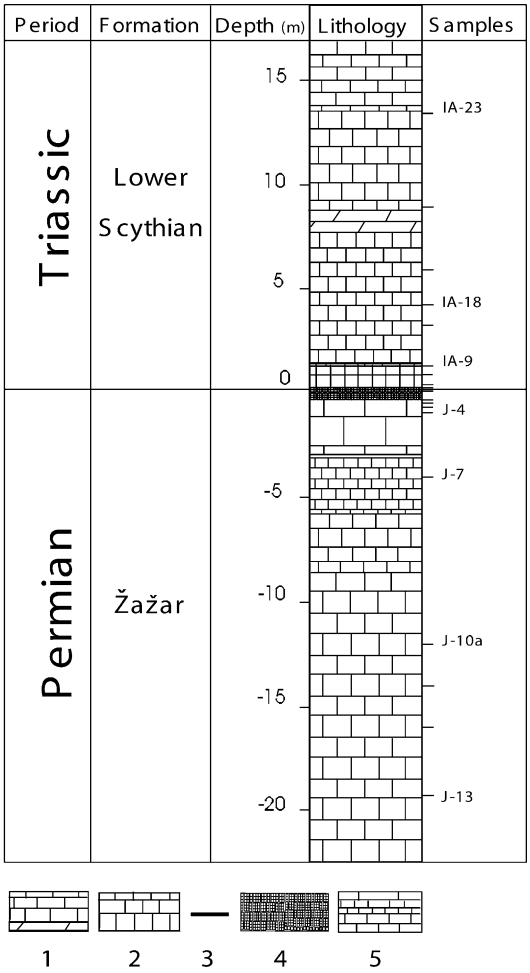

Fig. 2. Stratigraphic column of the P/Tr section studied in the Idrijca Valley, Slovenia (adapted from Dolenec et al., 2001). 1 = laminated dolomitic limestone alternating with grey stylolitic dolomites; 2 = well bedded sparitic limestone; 3 = P/Tr represented by 0.8 cm thick clayey marl layer; 4 = black algal packstone; 5 = limestone microfacies represented by packstones, grainstones and wackestones very rich in microfossils.

3. Samples and methods

Twenty fresh samples collected from 13.4 m above (+13.4) to 19.0 m below (−19.0) the P/Tr boundary in the Idrijca section (Fig. 2) were selected for organic geochemical analyses.

Descriptions of the samples are given in Dolenec et al. (2001). Additional petrographic examinations indicate that all the samples studied are nonmetamorphosed. The Upper Permian samples are laminated black packstones with abundant calcareous algae, foraminiferae, and some brachiopods. The samples around the P/Tr boundary are more sparitic. The sample 0.1 m above the boundary is an oolitic limestone. Some relics of reworked microfossils were observed in the uppermost Permian samples. The lowermost Scythian samples are grey well bedded sparitic limestones with detrital quartz and scarce microfossils. The uppermost Scythian samples are laminated mudstones.

To remove any superficial contamination from handling and weathered material, the rock samples were cut in slabs with a water cooled saw, washed with analytical grade and glass distilled acetone, ethanol, and water, and dried at 50 °C for 48 h. The cleaned samples were powdered in an agate ball-mill, and analyzed for distribution and isotopic composition of hydrocarbons according to the procedure described by Spangenberg and Macko (1998). Rock powders were submitted to total organic C (C_{org}) and Rock-Eval analysis at the Humble Geochemical Services Division (Humble, TX 77347).

Carbon and O isotope analyses were performed following the modified CO_2 extraction technique of McCrea (1950). Approximately 10 mg of the powdered carbonates were dissolved at 50 °C with 100% phosphoric acid. The released CO_2 was cryogenically purified, and measured in a Finnigan MAT Delta S isotope ratio mass spectrometer (IRM*S*). The stable C and O isotope ratios are reported in the delta (δ) notation as the per mil (‰) deviation relative to the Vienna Pee Dee Belemnite (VPDB) international standard. The analytical reproducibility, estimated from multiple analyses of the laboratory working standard Carrara marble, is better than ±0.05‰ for C ($\delta^{13}C_{carb}$) and ±0.1‰ for O ($\delta^{18}O_{carb}$).

Another aliquot of samples was then refluxed with an azeotropic mixture of dichloromethane and methanol (50/50, v/v) for 48 h, with change of solvent after the first 24 h. The extractable organic matter (EOM) was desulfurized with activated Cu (24 h, room temperature). The insoluble organic matter (kerogen) was obtained by acidification of the extracted sample with 6 N HCl. The oven-dried residues (consisting mostly of kerogen, little quartz and clay) and the bulk S-free EOM were analyzed for C-isotopic composition by using a Carlo Erba 1108 elemental analyzer (EA) connected to a Finnigan MAT Delta S IRMS via a Conflo II split interface (EA/IRM*S*). The reproducibility of the EA/IRMS analyses, monitored by replicate analyses of a laboratory working standard, was better than 0.1‰ for $\delta^{13}C_{EOM}$ and $\delta^{13}C_{ker}$.

The extracts were fractionated by silica-alumina liquid chromatography into aliphatic, aromatic and NSO compounds. Chemical characterization of the aliphatic hydrocarbons was performed with an Agilent Technologies 6890 GC coupled to an Agilent Technologies 5973 quadrupole mass selective detector (GC/MSD) using a HP-ULTRA-2 fused-silica capillary column (50 m × 0.20 mm i.d. coated with 0.11 μm cross-linked 5%-diphenyl–95%-dimethyl siloxane as stationary phase) and He as carrier gas. The samples were injected splitless at 280 °C. After an initial period of 7 min at 70 °C, the column was heated to 280 °C at 5 °C/min followed by an isothermal period of 20 min. The MSD was operated in the electron impact mode at 70 eV, source temperature of 250 °C, emission current of 1 mA and multiple-ion detection with a mass range from 50 to 700 amu. Compound identifications are based on comparison of standards, GC retention time, mass spectrometric fragmentation patterns and literature mass spectra.

The compound specific C isotope analyses of the aliphatic hydrocarbons were obtained by the use of an Agilent Technologies 6890 GC coupled to a Finnigan MAT Delta S IRMS by a combustion (C) interface III (GC/C/IRM*S*) under a continuous He flow (Hayes et al., 1990). The GC was operated with the same type of column and temperature program used for GC/MSD analyses. The CuO/NiO/Pt combustion reactor was set at 940 °C. The accuracy of the GC/C/IRMS measurements was monitored by co-injection of a laboratory standard (deuterated naphthalene) of known isotopic composition. The reproducibility was assessed by at least 3 replicate analyses of the Idrijca samples, and ranged between 0.05 and 0.5‰.

4. Results

4.1. Bulk geochemical data

4.1.1. Total organic carbon and Rock-Eval parameters

The average total organic C (C_{org}) content of the Idrijca samples (Table 1) is about 0.17 wt.%. The C_{org} content of the Upper Permian (0.24±0.06 wt.%) is higher than the Lower Scythian (0.14±0.04 wt.%) samples, and the lowest values (~0.1 wt.%) are found at the P/Tr and the lowermost Scythian samples (Fig. 3). A sharp increase in C_{org} combined to a C_{carb}-decrease at sediments ~14 m below the boundary indicates higher primary productivity (increased pCO_2 or other nutrients supply) and/or enhanced preservation of the organic matter sequestrated in the sediments.

The Rock-Eval pyrolysis data are used to assess temperature of maximum hydrocarbon generation (T_{max}), to indicate the degree of thermal maturity of the kerogen and to determine the hydrogen (HI) and oxygen (OI)

indices to chemically characterize the organic matter (e.g., Peters, 1986). The absence of Rock-Eval S_1 (free hydrocarbons) and S_2 (pyrolytic hydrocarbons) peaks in the Idrijca sample pyrolysates precludes the determination of the parameters T_{max}, HI and OPI (oil potential index), and kerogen-typing. This may be attributed to high thermal maturation, extensive oxidation, or bacterial degradation of the organic matter, combined with low initial organic matter contents. The OI values range from 0 to 275 mg CO_2/g C_{org} (Table 1). Because of high carbonate content and low organic matter content (Table 1), the whole-rock pyrolysis of Idrijca samples may give apparently high OI values due to interference of pyrolyzed carbonate-minerals (e.g., Whelan and Thompson-Rizer, 1993). Therefore, the OI values of Idrijca carbonates should be interpreted with caution. Nevertheless, the OI profile (Fig. 3) shows a sharp positive shift in the sediments ~0.7 m below the boundary, indicating enhanced oxidizing conditions at the top of the Upper Permian. The lowermost Scythian samples, ~0.3 m above the boundary, have a higher content in extracts (54.6–79.3 mg EOM/g C_{org}) compared to the Upper Permian samples (6.4±0.04 mg EOM/g C_{org}, Fig. 3).

4.1.2. $\delta^{13}C$ and $\delta^{18}O$ of carbonates

The $\delta^{13}C$ values of the carbonates from the Idrijca section vary between −0.5 and +4.6‰, while the $\delta^{18}O_{carb}$ values cover a narrower range, from −8.1 to −5.1‰ (Table 1). The relatively high $\delta^{13}C$ values are typical of marine carbonates (e.g., Anderson and Arthur, 1983). The stratigraphic $\delta^{13}C_{carb}$ profile shows a ^{13}C-decrease of up to 5‰ at the transition from the uppermost Permian grey-black packstones/grainstones to the earliest Triassic light grey sparitic limestones (Fig. 4). Previous carbonate C isotopic investigations of the Idrijca Valley section display a comparable $\delta^{13}C_{carb}$ excursion of +4‰ in the beds of the Žažar Formation to −1‰ in the Lower Triassic beds (Baud et al., 1989; Dolenec et al., 2001). The $\delta^{13}C_{carb}$ declines gradually from +4.6‰ at the Žažar Formation lowermost sample to about +3‰ near the boundary level (Fig. 4). The $\delta^{13}C_{carb}$ shift across the boundary is rather abrupt. The $\delta^{13}C_{carb}$ values drop from ~2.9‰ about 1.2 m below the P/Tr boundary to 1.2‰ at the boundary level. The Lower Scythian rocks are relatively depleted with $\delta^{13}C_{carb}$ of about −0.5‰. Similar gradual decrease of more than 4‰ from Upper Permian to Lower Scythian beds has been reported in numerous Tethyan sections in the Southern Alps (Baud et al., 1989) and worldwide (Magaritz et al., 1992, and references therein).

4.1.3. $\delta^{13}C$ of kerogens and rock-extracts

The C-isotope composition of the kerogens (−30.0 to −25.4‰, Table 1, Fig. 4) isolated from the Idrijca section sediments are similar to the values for total organic

Table 1
Results of Rock-Eval OI parameter[a] and stable isotope analyses of carbonates ($\delta^{13}C_{carb}$, $\delta^{18}O_{carb}$), kerogens ($\delta^{13}C_{ker}$) and extracts ($\delta^{13}C_{EOM}$) of samples from the Permian–Triassic section at Idrijca Valley

Field no.	Lab. no.	Depth[b] (m)	C_{org} (wt.%)	C_{carb} (wt.%)	OI	$\delta^{13}C_{carb}$ (‰, VPDB)	$\delta^{18}O_{carb}$ (‰, VPDB)	$\delta^{13}C_{ker}$ (‰, VPDB)	EOM (mg/g C)	$\delta^{13}C_{EOM}$ (‰, VPDB)
IA-23	VS-1	13.4	0.13	95.13	54	−0.5	−7.5	−28.7	6.7	−26.5
IA-22	VS-1a	8.9	0.16	94.85	35	−0.3	−5.1	−28.7	4.4	–
IA-21	VS-1b	5.9	0.18	88.22	56	0.2	−5.3	−30.0	139	−26.5
IA-18	VS-1c	4.3	0.23	95.60	63	0.2	−7.3	−29.7	34.0	–
IA-17	VS-2	3.3	0.11	91.83	73	0.1	−7.5	−27.0	1.4	−28.3
IA-9	VS-3	1.2	0.10	97.35	20	0.5	−7.1	−27.1	3.6	−29.3
IA-7	VS-4	0.7	0.11	96.35	18	0.7	−7.4	−25.7	8.2	−24.3
IA-4/5	VS-5	0.3	0.10	97.52	0	0.9	−7.2	−25.4	79.0	−26.7
IA-3	VS-6	0.1	0.16	84.94	31	1.2	−7.6	−25.9	54.0	−26.2
IA-1/2	VS-7	0.0	0.17	82.66	0	1.2	−7.6	−26.1	22.0	−26.1
Joa/b	VS-8	−0.1	0.14	96.21	57	1.2	−7.8	−26.0	13.6	−27.6
J-2b	VS-9	−0.6	0.17	87.47	247	2	−7.2	−26.7	10.8	−26.2
J-3b	VS-10	−0.7	0.20	92.10	275	2.4	−7.6	−27.6	13.7	−27.2
J-3a	VS-11	−0.9	0.24	90.09	79	2.3	−7.8	−27.9	7.1	−26.6
J-4	VS-12	−1.2	0.28	90.06	82	2.9	−8.1	−28.4	0.4	−26.4
J-7	VS-13	−4.1	0.27	93.09	30	4	−7.2	−27.4	0.8	−27.8
J-10a	VS-14	−12.5	0.21	92.00	14	4.3	−6.7	−26.4	7.0	−26.7
J-11	VS-15	−14.0	0.34	79.34	35	4.4	−6.8	−26.6	5.9	–
J-12	VS-16	−16.0	0.26	92.09	54	4.5	−6.4	−26.5	3.5	−26.5
J-13	VS-17	−19.0	0.23	95.68	52	4.6	−6.6	−26.7	4.8	–

[a] Rock-Eval OI = oxygen index ($S_3 \times 100$/TOC, mg CO_2/g C_{org}).
[b] Depth = distance to the P/Tr boundary; – not analyzed.

C ($\delta^{13}C_{org} = -29.3$ and -25.1‰) reported by Dolenec et al. (2001). The wide range (4.6‰) is most likely due to variations in primary composition of the organic matter (i.e. variable contribution from marine plankton, bacteria, algae and land plants) and variations in productivity rate during deposition. The $\delta^{13}C_{ker}$ values of the Upper Permian kerogens are fairly uniform (-26.7 ± 0.8‰), with a minimum of -28.4‰ at -1.2 m, and less negative than the Scythian samples $> +1.2$ m (-28.7 ± 1.2‰). The $\delta^{13}C_{org}$ values of the closely spaced samples set studied by Dolenec et al. (2001) show that the ^{13}C-depletion begins about 50 cm below the boundary, with a minimum value of -29.3‰ at the boundary level. The shift from the Upper Permian values to the Lower Scythian is up to -3.6‰ (Fig. 4). A positive $\delta^{13}C_{ker}$-shift occurs in the earliest Scythian samples up to 0.7 m above the boundary with a maximum of -25.4‰ at $+0.3$ m. Above this level, a decreasing trend of the $\delta^{13}C_{ker}$ of the Triassic samples begins, with a minimum value of -30‰ about 5.9 m above the boundary (Fig. 4).

The Idrijca sediments contain low amount of extractable organic matter (0.4–139 mg EOM/g C). The $\delta^{13}C$ values (-28.3 to -24.3‰) of the extracts generally differ less than ± 2‰ from the $\delta^{13}C$-value of the associated kerogen, except for 2 Lower Scythian samples (more than ~4.3 m above the boundary) with $\Delta_{EOM\text{-}ker}$ up to 3.5‰ (Table 1). The extracts are usually isotopically

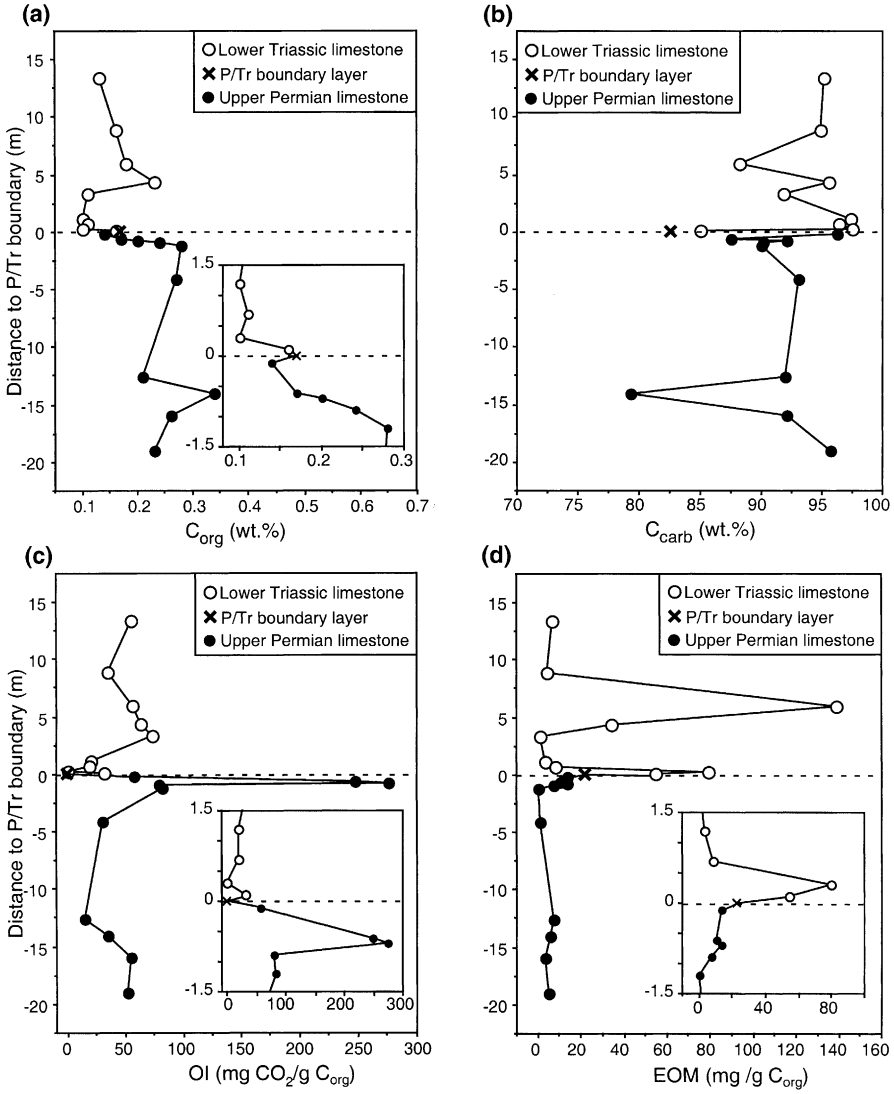

Fig. 3. Stratigraphic profiles of organic (a) and carbonate (b) carbon contents, oxygen index (c) and extract content (d) in samples from the P/Tr section at Idrijca Valley.

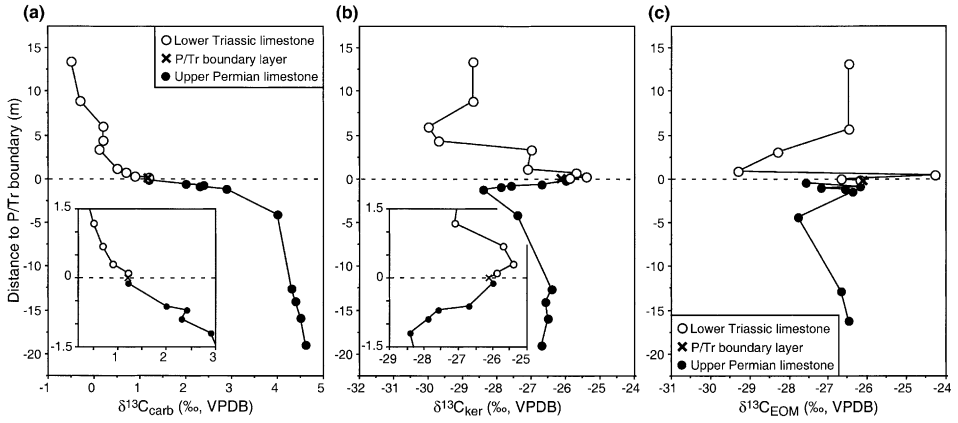

Fig. 4. Stratigraphic profiles of C isotope composition of carbonates (a), kerogen (b) and extract (c) in samples from the P/Tr section at Idrijca Valley.

lighter than the source kerogen (e.g., Stahl, 1978). The $\delta^{13}C_{EOM} \leqslant \delta^{13}C_{ker}$ values (Table 1) are consistent with an indigenous origin for the lipids from Idrijca sediments. During migration, water-washing, thermal maturation, and chemical or biological degradation, the free hydrocarbons may lose isotopically light moieties (e.g., Engel et al., 1991; Palmer, 1993). Consequently the residual hydrocarbons are depleted in ^{12}C, and the extract may be isotopically heavier than the associated kerogen. The extracts from the uppermost Permian sediments (>-1.2 m; samples J-2b, J-3b, J-3a, J-4) are isotopically heavier (up to 2‰) than the associated kerogen, suggesting a contribution of (locally) migrated hydrocarbons (Table 1). This ^{13}C enrichment supports the Rock-Eval OI results, indicating an enhanced alteration (oxidation) of the organic matter in the uppermost Permian sediments.

4.2. Molecular geochemical data

4.2.1. Hydrocarbons distribution

Normal alkanes, acyclic isoprenoids, branched alkanes, and alkylcyclohexanes are the main extractable compounds (Fig. 5). High amounts of unresolved complex mixtures (UCM) of alkanes are generally present in the GC traces of all the samples.

The distribution of *n*-alkanes ranges in C-chain length from C_{11} to C_{35} and shows an odd to even C number predominance (CPI range from 0.9 to 2.6, average = 2.0). The most abundant *n*-alkanes vary widely from C_{17}–C_{29} (Table 2). The Upper Permian *n*-alkanes range between C_{11} and C_{35}, maximizing around C_{17} to C_{21}. The predominance of low molecular weight compounds maximizing at C_{17} or C_{18} is typically attributed to algae and cyanobacteria (Hunt, 1996 and references therein). Long-chain *n*-alkanes with an odd-over-even predominance are generally attributed to higher plants (Eglinton and Hamilton, 1963). High concentrations of these homologues can also be derived from reduction of C_{25}–C_{31} alkenes of the freshwater green microalga *Botryococcus braunii* (Metzger and Casadewall, 1991). Additionally, *B. braunii* is characterized by an unusually high lipid content (Grice et al., 1998 and references therein). The high CPI ratios of long-chain *n*-alkanes and high lipid content of the samples 0.1–0.7 m above the boundary argue for a more algal (e.g., *B. braunii*) and/or higher plants contribution to the organic matter in the lowermost Scythian sediments (Table 2). The *n*-alkanes in the sediments around −0.6 m (samples J-2b), +0.1 m (sample IA-3) and +5.9 m (sample IA-21) from the boundary show bimodal distributions maximizing at C_{17}–C_{29}, C_{20}–C_{25} and C_{18}–C_{24} respectively. This indicates the variability of bacterial, algal, and higher plants contributions, probably due to changes in the phytoplanktonic productivity in the Permian–Triassic water column.

Acyclic isoprenoids occur in the range C_{18}–C_{30}. The isoprenoids pristane (Pr, C_{19}) and phytane (Ph, C_{20}) can be derived from the phytol side-chain of chlorophyll in aerobic phototrophic organisms as algae and cyanobacteria. Didyk et al. (1978) suggested that low Pr/Ph-ratios (Pr/Ph <1) indicate anoxic conditions, whereas higher Pr/Ph ratios (>1) oxic conditions. The higher Pr/Ph ratios ($\geqslant 1$) in the ~ -0.9 to $+3.3$ m samples suggest an oxic depositional environment during the P/Tr transition (Table 2). However, this ratio is known to be strongly influenced by source variation, migration and biodegradation effects (e.g., ten Haven et al., 1987). The range of values for the Pr/*n*-C_{17} (0.4 to 1.3), Ph/*n*-C_{18} (0.2 to 1.0) and Pr/Ph (0.2 to 2.1) concentration ratios might reflect differences in the depositional environment of the organic sources, superimposed by changes caused by differences in maturity, biodegradation and mineralization effects. Small amounts of C_{21}–C_{30} acyclic isoprenoids are present in all samples. The C_{21}–C_{25} acyclic isoprenoids were suggested as biomarkers of a lagoonal-type, saline environment, being derived from

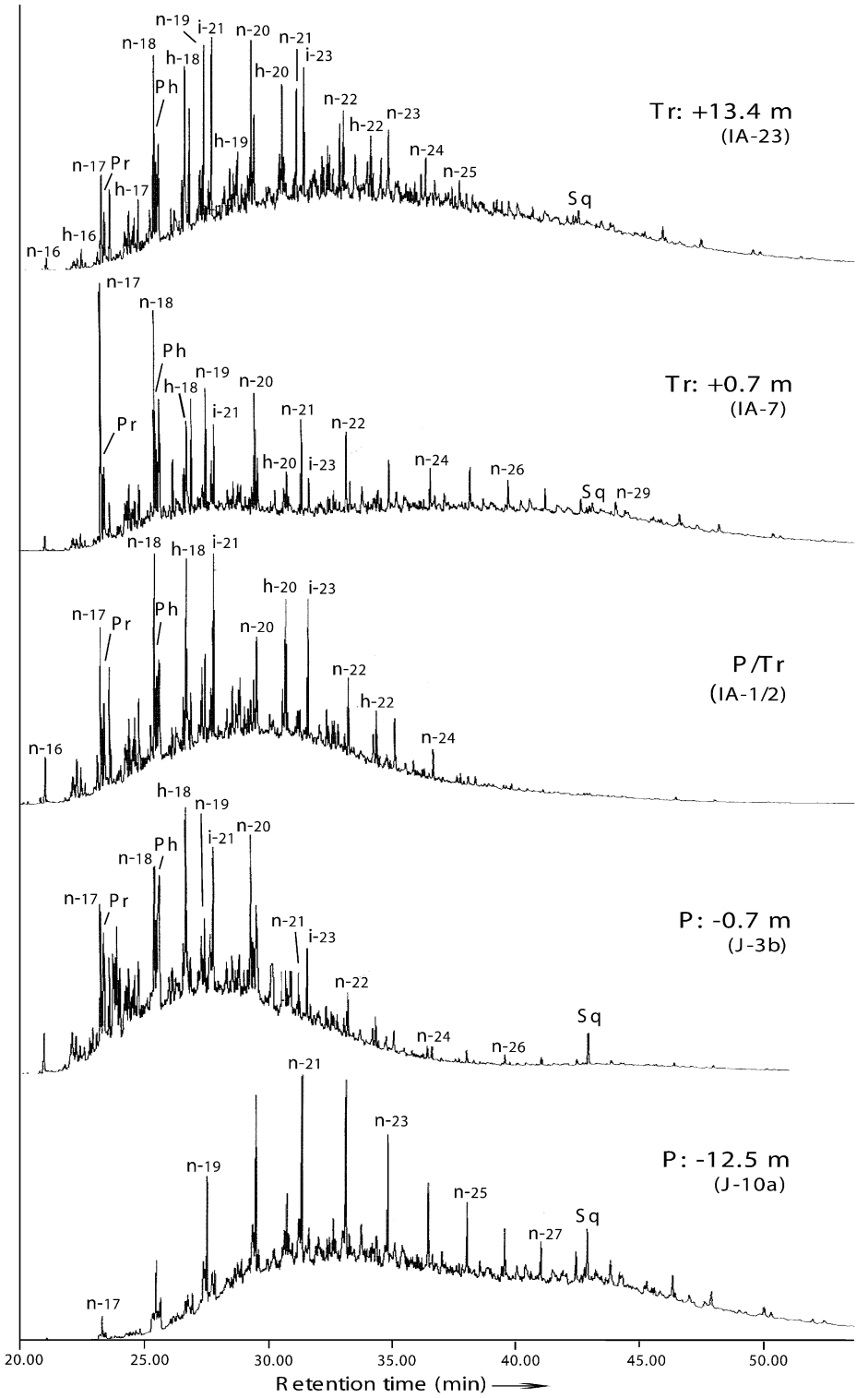

Fig. 5. GC–MS TIC traces of the saturated hydrocarbon fractions from samples across the Permian–Triassic transition at Idrijca Valley. n-x = normal alkane, h-x = alkylcyclohexane and i-x = isoprenoid with x carbon atoms; Pr = pristane; Ph = phytane; Sq = squalane.

Table 2
Distribution of hydrocarbons and biomarker parameters of saturated fractions of samples from the Permian–Triassic section at Idrijca Valley

Field no.	Depth (m)	*n*-Alkanes (maxima)	Pr/Ph	Pr/*n*–C_{17}	Ph/*n*–C_{18}	CPI C_{22}–C_{30}	Acyclic isoprenoids	Alkyl-cyclohexanes	CPIM	Ster/hop	Steranes			Sq
											% C_{27}	% C_{28}	% C_{29}	
IA-23	13.4	C_{15}–C_{32} (C_{18})	0.81	0.86	0.46	2.41	C_{19}, C_{20}, C_{22}, C_{24}	C_{16}–C_{28} (C_{18})	3.36	2.4	42.3	26.3	31.4	0.5
IA-21	5.9	C_{11}–C_{32} (C_{18}, C_{24})	0.16	0.55	0.76	1.64	C_{19}, C_{20}, C_{22}, C_{24}	C_{15}–C_{32}(C_{21})	1.28	1.3	41.2	25.8	33.0	0.6
IA-18	4.3	C_{16}–C_{25} (C_{20})	0.81	1.30	1.00	1.93	C_{19}, C_{20}, C_{22}, C_{24}	C_{16}–C_{26} (C_{17})	0.73	0.4	42.1	31.5	26.4	ni
IA-17	3.3	C_{16}–C_{31} (C_{18})	1.41	0.73	0.43	2.22	C_{19}, C_{20}, C_{22}	C_{16}–C_{27} (C_{18})	1.30	1.0	35.8	30.5	33.7	0.4
IA-9	1.2	C_{16}–C_{29} (C_{22})	2.09	0.67	0.25	0.89	C_{19}, C_{20}, C_{22}	C_{16}–C_{25} (C_{21})	1.45	3.8	50.4	31.3	18.3	0.3
IA-7	0.7	C_{16}–C_{30} (C_{17})	1.64	0.43	0.37	2.65	C_{19}, C_{20}, C_{22}, C_{24}, C_{26}, C_{28}	C_{16}–C_{28} (C_{18})	0.98	1.5	42.5	27.1	30.4	0.7
IA-4/5	0.3	C_{16}–C_{31} (C_{18})	1.82	0.63	0.40	2.59	C_{18}, C_{19}, C_{20}, C_{22}, C_{24}	C_{16}–C_{25} (C_{18})	1.17	0.8	39.7	25.9	34.4	1.8
IA-3	0.1	C_{16}–C_{31} (C_{20}, C_{25})	0.99	0.87	0.48	2.27	C_{19}–C_{29}	C_{18}–C_{28} (C_{21})	1.58	1.5	41.2	28.1	30.7	2.1
IA-1/2	0.0	C_{16}–C_{27} (C_{18})	1.08	0.89	0.53	1.81	C_{18}–C_{24}	C_{16}–C_{25} (C_{18})	1.39	0.6	49.4	20.5	30.1	ni
Joa/b	−0.1	C_{16}–C_{26} (C_{18})	0.99	0.87	0.49	1.79	C_{19}–C_{22}, C_{24}	C_{16}–C_{26} (C_{18})	1.37	0.8	40.4	27.0	32.6	ni
J-2b	−0.6	C_{11}–C_{35} (C_{17}, C_{29})	1.29	0.77	0.56	1.71	C_{19}–C_{30}	C_{16}–C_{28} (C_{18})	2.91	1.1	31.0	31.8	37.2	1.8
J-3b	−0.7	C_{16}–C_{31} (C_{18})	1.57	1.19	0.65	2.15	C_{19}–C_{22}	C_{16}–C_{26} (C_{18})	1.49	0.8	35.2	29.1	35.7	0.9
J-3a	−0.9	C_{16}–C_{29} (C_{18})	2.07	0.62	0.20	1.93	C_{19}–C_{22}, C_{24}	C_{16}–C_{25} (C_{18})	1.46	ni	ni	ni	ni	1.3
J-10a	−12.5	C_{16}–C_{32} (C_{21})	0.22	0.41	0.50	1.87	C_{19}–C_{22}, C_{24}	C_{17}–C_{25} (C_{21})	1.39	1.1	37.1	25.0	37.9	0.9
J-12	−16.0	C_{16}–C_{29} (C_{18})	1.01	1.02	0.36	1.85	C_{19}, C_{20}, C_{22}, C_{24}–C_{26}	C_{16}–C_{25} (C_{19})	1.06	1.5	29.9	32.1	38.0	1.9

CPI = Carbon Preference Index for *n*-alkanes = 2∑odd (C_{23}–C_{29})/[∑even (C_{22}–C_{28}) + ∑even (C_{24}–C_{30})]; Pr = pristane; Ph = phytane; C_x = alkane with *x* carbon atoms; ni = not identified; CPIM = Carbon Preference Index for alkylcyclohexanes = 0.5[(C_{19}–C_{25})/(C_{18}–C_{24}) + (C_{19}–C_{25})/(C_{20}–C_{26})]; Ster/hop = ∑(C_{27}–C_{29}) steranes (*m*/*z* 217)/∑(C_{27}–C_{32}) hopanes (*m*/*z* 191); %C_{27} steranes = [∑(ααα + ααβ C_{27}) steranes/∑(ααα + ααβ C_{27}–C_{29}) steranes]; sq = % area of squalane.

halophilic archaea (Waples et al., 1974). Longer chained acyclic isoprenoids (C_{25+}) in samples +0.7, +0.1 and −0.6 and −16.0 from the boundary (Table 2) may originate by thermal degradation of the C_{40} isoprenoid identified in the freshwater alga *B. braunii* (e.g., Höld et al., 1998). Moreover significant amounts of squalane are detected in almost all the samples (Table 2). The olefin of squalane (squalene) is common in most marine organisms and higher plants, and is not a specific biomarker (Hunt, 1996; Sukh Dev, 1989). It was reported that *B. braunii* biosynthesizes epoxides of polymethylated squalenes (Metzger and Aumelas, 1997). Therefore, the relatively higher abundance of squalane in samples with C_{25+} isoprenoids may suggest a *B. braunii* contribution to the organic matter in these sediments.

The distribution of alkylcyclohexanes ranges between C_{15} and C_{32}, maximizing around C_{18} and C_{21} for Upper Permian and Scythian samples, respectively (Table 2, Fig. 6). Alkylcyclohexanes can be formed by decarboxylation of cyclic fatty acids of algal or bacterial origin (Rubinstein and Strausz, 1979; Schulze and Michaelis, 1990). The algal cyclic fatty acids have an even number of C atoms (e.g., Hoffman et al., 1987), and the bacterial cyclic fatty acids an odd number of C's (mainly thermoacidophilic bacteria, Fowler et al., 1986; Hoffman et al., 1987). Therefore, decarboxylation of cyclic fatty acids of algal or bacterial origin will give alkylcyclohexanes with an odd to even predominance, respectively. Only two Scythian samples (∼+0.7 and +4.3 m) have a clear even C-number predominance (CPIM = 0.98 and 0.73), which may indicate a major contribution of bacterial biomass to the predominantly algal organic matter (Table 2). The odd-over-even C-number predominance of alkylcyclohexanes ranging from C_{16}–C_{28} (CPIM up to 3.36) maximizing around C_{18}–C_{22} (Table 2) supports a substantial algal contribution to the Permian and uppermost Triassic samples.

A series of alkylcyclopentanes from C_{15} to C_{26}, maximizing around C_{18} and C_{21} were detected in the *m*/*z* 69 ion chromatograms of all samples (Fig. 7). It has been suggested that these compounds have been formed by cyclization of unsaturated fatty acids during diagenesis (Philp, 1980). The distribution of the alkylcyclopentanes shows roughly similar patterns as those of alkylcyclohexanes. This suggests that these alkylcycloalkanes have been formed via a similar pathway, i.e. cyclization of straight-chain fatty acids (Rubinstein and Strausz, 1979).

Hopanes in the range C_{27}–C_{34}, with predominances of C_{29} and C_{30}, and 17α,21β(H) configuration were detected in the *m*/*z* 191 ion chromatograms of all samples. The C_{32+} hopanes are present in trace amounts. Hopanes in saturated hydrocarbon fractions of sediments are derived from bacteria, and steranes from algae and higher plants (e.g., Peters and Moldowan, 1993). A series of steranes in the range C_{27}–C_{29}, maximizing at C_{27}, were detected in all the samples (Table 2, Fig. 8). The sterane/hopane ratios scatter between 0.4 and 3.8 (Table 2), indicating fluctuations in the contribution of algae and bacteria to the sedimentary biomass. The higher concentrations of C_{27} steranes compared to the C_{28} and C_{29} homologues in all the samples point to a marine input (Peters and Moldowan, 1993 and references therein). Significant levels of C_{29} steranes may also indicate a contribution of land plants (e.g., Czochanska et al., 1988). Small changes in the concentrations of C_{29} steranes reflect a continuous contribution of terrestrial plants in the P/Tr boundary and Lower Scythian sediments in the Idrijca section (Fig. 8).

4.2.2. $\delta^{13}C$ of the individual alkanes

Seven samples contained sufficient amounts of the saturated fraction for accurate compound specific C-isotopic analyses of *n*-alkanes, pristane and phytane. The $\delta^{13}C$ values of the measured alkanes range from −27.2 to −31.6‰ (Table 4, Fig. 9). The C_{16}–C_{23} *n*-alkanes of the <-0.9 m Upper Permian samples are enriched in ^{13}C by up to 2.5‰ relative to the uppermost >-0.7 m samples, having average values of -27.7 ± 0.4‰ and -30.2 ± 0.7‰, respectively. In the uppermost Permian (−0.1 m) and lowermost Scythian samples (+0.3 m) the C_{16}–C_{20} *n*-alkanes, maximizing at C_{18}, are slightly depleted in ^{13}C relative to the C_{21}–C_{31} homologues within the same sample (Fig. 9). These differences in $\delta^{13}C$ values of the short chain *n*-alkanes may indicate the different biological source of these compounds or different primary productivity. In most samples the $\delta^{13}C$ values of pristane and phytane are similar (−28 to −31‰), although Pr is more depleted in ^{13}C (up to 1.4‰) in the Upper Permian samples (Table 4). This close similarity in $\delta^{13}C$ values indicates a common origin (e.g., algae, cyanobacteria, phototrophic bacteria) for Pr and Ph. In the Upper Permian (∼−0.9 m) and the lowermost Scythian (∼+0.3 m) sediments Pr (∼−30.5‰) and Ph (∼−29.6‰) are isotopically lighter by up to 2.9‰ relative to the associated *n*-alkanes (Fig. 9). In the Lower Triassic samples (∼+1.2 m), the Pr and Ph are enriched in ^{13}C by ∼2.5‰ relative to the *n*-alkanes. The isoprenoid lipids are generally depleted by ∼0.5‰ (Freeman et al., 1994) relative to the *n*-alkanes of the same biological precursor. Therefore, the much-greater ^{13}C-depletion of both Pr and Ph compared to the C_{17} *n*-alkanes in the Upper Permian samples suggests that these compounds may not be derived from the same primary producers as the *n*-alkanes (see below).

5. Discussion

5.1. Organic matter sources

The changes in the marine organic matter content and isotopic composition reflect changes in the contributions

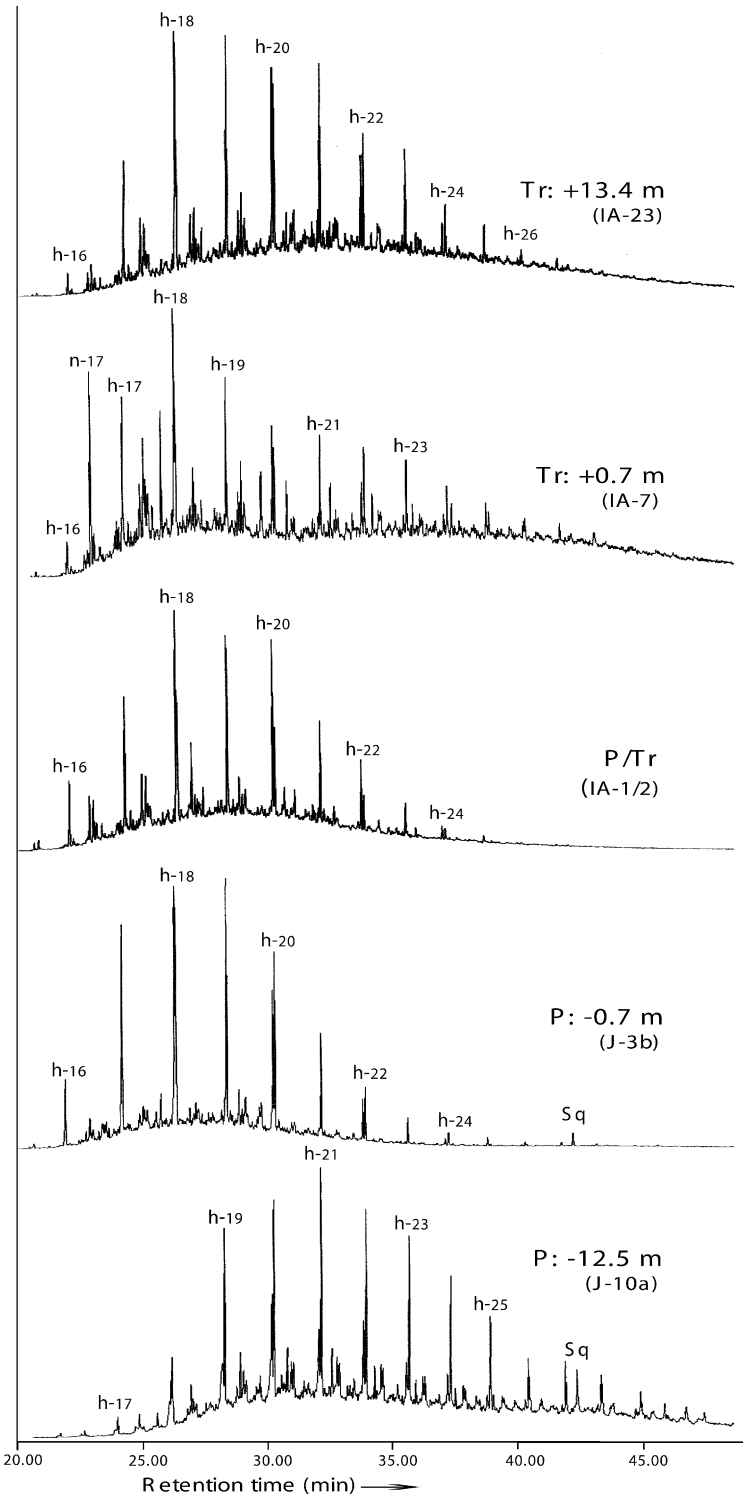

Fig. 6. Ion chromatograms of $m/z = 82–83$ showing the distribution of alkylcyclohexanes of the saturated hydrocarbon fractions from samples across the Permian–Triassic transition at Idrijca Valley. Abbreviations as in Fig. 5.

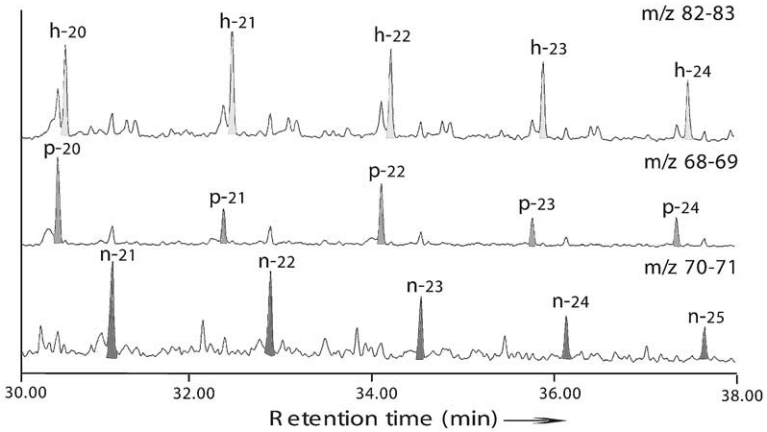

Fig. 7. Expanded ion chromatograms of $m/z = 82–83$ for alkylcyclohexanes (h-x), $m/z = 68–69$ for alkylcyclopentanes (p-x), and $m/z = 70–71$ for n-alkanes (n-x) in the Permian sediment J-10a.

of different organic sources, the primary productivity in the water column, and the availability and speciation of dissolved inorganic C (DIC) used as nutrient by photosynthetic organisms (e.g., Hollander and McKenzie, 1991; Fogel and Cifuentes, 1993). The distribution of alkanes in the Idrijca sediments suggests main contributions from algae (predominance of mid chain n-alkanes, odd C-number alkylcyclohexanes, C_{27} steranes) and bacteria (predominance of hopanes over steranes). The higher abundances of odd long-chain n-alkanes in the range C_{25}–C_{31} suggest higher terrestrial contributions to the organic matter at the P/Tr transition and lowermost Scythian samples. The relatively heavy kerogens (in ^{13}C content) and long-chain n-alkanes support higher contributions of terrestrial plant detritus to the marine organic matter. This merits a further explanation. Unlike the isotopic records for the modern biogeochemical C cycle, the terrigenous organic matter in pre-Miocene time was isotopically heavier relative to marine organic matter (e.g., Arthur et al., 1985; Popp et al., 1989). Thus, the ^{13}C-enrichment of the bulk organic components (kerogens, extracts) at the Idrijca sediments from ~ -0.1 to $+0.7$ m of the P/Tr transition could be attributed to a minor input of higher plants.

5.2. Paleoenvironmental interpretation

The Upper Permian Žažar Formation was deposited under euxinic conditions where water-column circulation was sluggish and recycling of organic matter was limited. This interpretation, based on geochemical data, is supported by sedimentological and paleontological data published by Ramovš (1986), which indicate that the laminated dark wackestones of the Žažar Formation were deposited in a quiet water environment under anoxic conditions. In contrast, the uppermost Permian (~ -0.9 m) to lowermost Scythian ($\sim +0.7$ m) sediments were deposited under oxygenated conditions, where circulation in the water body was strong and recycling of organic matter more efficient. The laminations of the uppermost Scythian samples indicate lack of burrowing organisms, suggesting a low dissolved-O_2 content at the water–sediment interface.

Anoxic conditions were more prevalent during deposition of the Upper Permian sediments, as suggested by the relatively higher C_{org} content and lower OI values. The high contents in whole rock S (Dolenec et

Table 3
Identified steranes in the saturated hydrocarbon fraction

Peak	Compound
a	C_{27} 13β(*H*),17α(*H*) (20*S*) diasterane
b	C_{27} 13β(*H*),17α(*H*) (20*R*) diasterane
c	C_{27} 13α(*H*),17β(*H*) (20*S*) diasterane
d	C_{27} 13α(*H*),17β(*H*) (20*R*) diasterane
e	C_{28} 13β(*H*),17α(*H*) (20*S*) diasterane
f	C_{28} 13β(*H*),17α(*H*) (20*R*) diasterane
g	C_{28} 13α(*H*),17β(*H*) (20*S*) diasterane
h	C_{27} 5α(*H*),14α(*H*),17α(*H*) (20*S*) sterane
i	C_{27} 5α(*H*),14β(*H*),17β(*H*) (20*R*) sterane
j	C_{27} 5α(*H*),14β(*H*),17β(*H*) (20*S*) sterane
k	C_{27} 5α(*H*),14α(*H*),17α(*H*) (20*R*) sterane
l	C_{29} 13α(*H*),17β(*H*) (20*S*) diasterane
m	C_{29} 13α(*H*),17β(*H*) (20*R*) diasterane
n	C_{28} 5α(*H*),14α(*H*),17α(*H*) (20*S*) sterane
o	C_{28} 5α(*H*),14β(*H*),17β(*H*) (20*R*) sterane
p	C_{28} 5α(*H*),14β(*H*),17β(*H*) (20*S*) sterane
q	C_{30} diasterane
r	C_{28} 5α(*H*),14α(*H*),17α(*H*) (20*R*) sterane
s	C_{29} 5α(*H*),14α(*H*),17α(*H*) (20*S*) sterane
t	C_{29} 5α(*H*),14β(*H*),17β(*H*) (20*R*) sterane
u	C_{29} 5α(*H*),14β(*H*),17β(*H*) (20*S*) sterane
v	C_{29} 5α(*H*),14α(*H*),17α(*H*) (20*R*) sterane

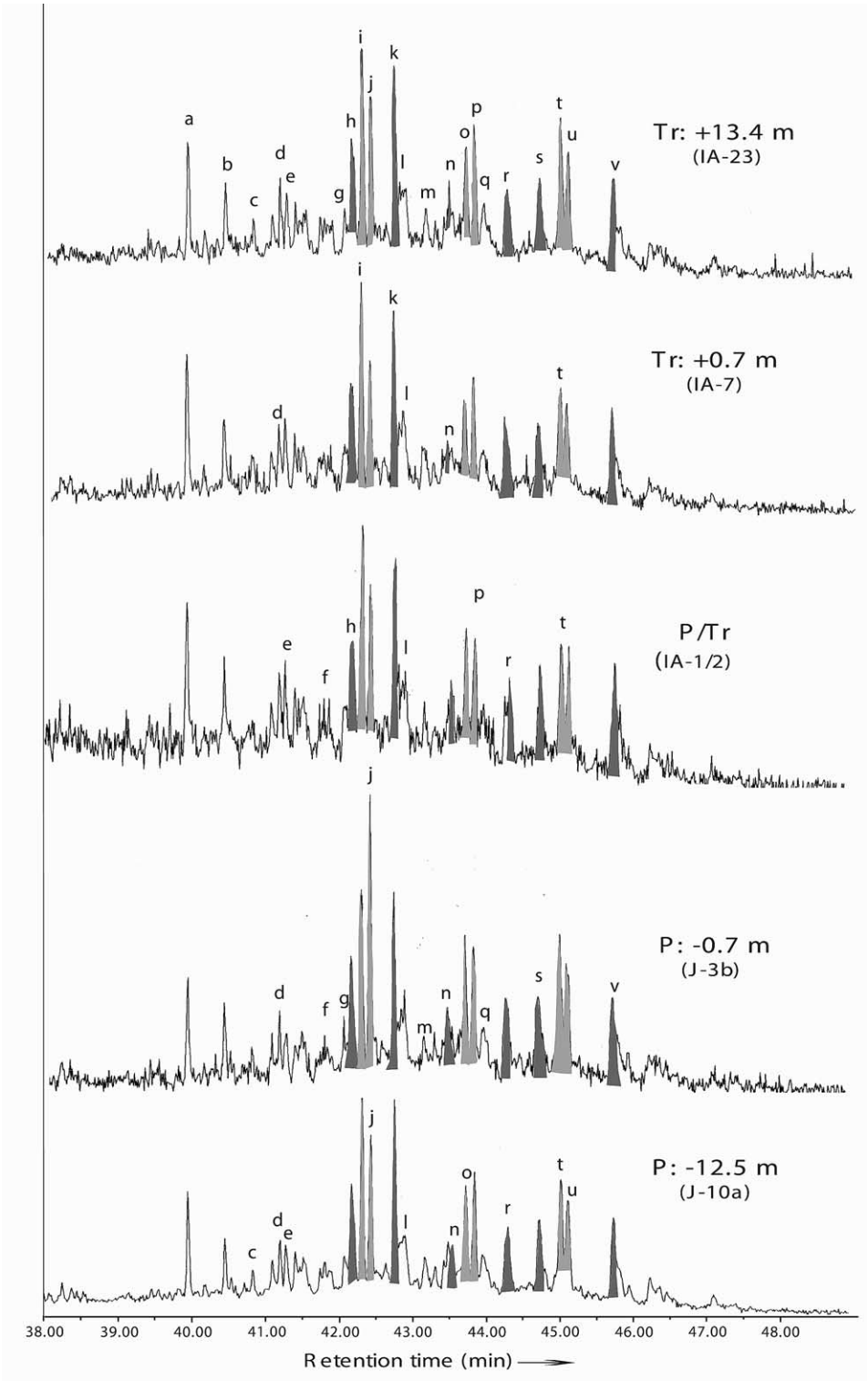

Fig. 8. Expanded mass chromatograms of $m/z = 217$ showing the distribution of steranes in samples from the P/Tr section at Idrijca Valley. Identification of labeled compounds is given in Table 3.

al., 2001) and extractable molecular S (S_8) in the Permian samples may point to an euxinic depositional environment (i.e. characterized by toxic H_2S-rich bottom waters). The high $\delta^{13}C$ values of kerogens, *n*-alkanes, and carbonates suggest enhanced productivity of phytoplankton biomass in the lowermost Permian samples (Table 1). In high productivity regimes, intense photosynthesis by primary producers consumes surface-water CO_2 and other nutrients. This may force some phytoplankton to pump HCO_3^-, causing a ^{13}C-enrichment in the marine biomass (Fogel and Cifuentes, 1993). In the samples ~−0.9 m below the P/Tr boundary the

Table 4
$\delta^{13}C$ values of *n*-alkanes (*n*-C_x, x = number of carbons) and isoprenoids (pristane, phytane) in samples of the P/Tr section at Idrijca Valley

Compound	$\delta^{13}C$ (‰, VPDB)						
	Permian				Triassic		
	−12.5 (J-10a)	−0.9 (J-3a)	−0.7 (J-3b)	−0.1 (Joa/b)	+0.3 (IA-4/5)	+1.2 (IA-9)	+3.2 m (IA-17)
n-C_{15}	–	–	–	−29.9		−29.7	–
n-C_{16}	–	–	−29.2	−29.7	−28.7	−29.2	–
n-C_{17}	–	−27.4	−30.0	−30.4	−29.2	−30.4	−28.0
Pr	–	−30.5	−31.3	−30.9	−30.4	−28.4	−30.5
n-C_{18}	−28.2	−27.6	−29.6	−31.3	−30.7	−29.4	−31.6
Ph	−29.4	−29.3	−29.9	−30.5	−29.8	−29.4	−30.7
n-C_{19}	−28.4	−28.1	–	−30.3	−29.6	−28.8	–
n-C_{20}	−27.5	−27.2	–	−31.2	−29.1	−28.3	–
n-C_{21}	−28.2	−27.5	–	–	−28.0	−29.6	–
n-C_{22}	–	−27.5	–	–	−28.1	−29.5	–
n-C_{23}	–	−27.4	–	–	–	–	–
n-C_{24}	–	–	–	–	−28.1	–	–
n-C_{25}	–	–	–	–	−27.2	–	–
n-C_{26}	–	–	–	–	−27.7	–	–
n-C_{27}	–	–	–	–	−27.9	–	–
n-C_{28}	–	–	–	–	−27.9	–	–
n-C_{29}	–	–	–	–	−28.5	–	–
n-C_{30}	–	–	–	–	−28.3	–	–
n-C_{31}	–	–	–	–	−28.5	–	–

– Not analyzed.

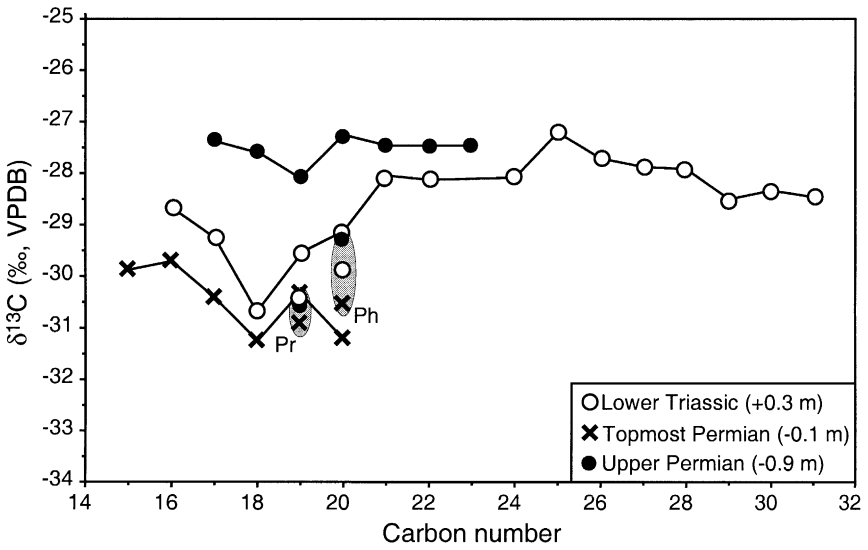

Fig. 9. $\delta^{13}C$ values of *n*-alkanes, pristane and phytane in samples from the P/Tr section at Idrijca Valley.

C_{17} *n*-alkane is significantly enriched in ^{13}C relative to pristane and phytane, suggesting that this compound is derived from a specific primary producer enriched in ^{13}C relative to the other primary producers. The ^{13}C-enriched source is most likely algae growing in the oxygenated photic zone (e.g., Guthrie, 1996). Decreases in organic C and carbonate contents, Pr/Ph ratios, increase of O indices, and ^{13}C-enrichment in kerogen, extracts and *n*-alkanes indicate a decrease of anoxia in the uppermost Permian bottom water. This is in line with the distribution of redox-sensitive trace elements (Mo, U, Cr and V) and the change of sign of the Ce anomaly (Dolenec et al., 2001), which argue for a transition from Upper Permian oceanic anoxia to an O_2-rich environment at the P/Tr transition. The ^{13}C-enrichment in kerogen, the high amount of extract, the predominance of C_{17} *n*-alkane with $\delta^{13}C$ values $\sim -30‰$ in the lowermost Scythian indicate substantial algal productivity. A contribution of the freshwater alga *B. braunii* is probably consistent with the higher contents of squalane and long chained acyclic isoprenoids (C_{25+}) in these samples. The predominance of odd long-chain *n*-alkanes enriched in ^{13}C (up to 4‰) indicates a contribution of higher land plants.

It is generally accepted that during a transgression phase, the nutrient supply to the water column is relatively high due to reworking of underlying sediments and input of weathered debris (e.g., Wolf et al., 1989). These conditions are favorable for high phytoplanktonic productivity. Furthermore, changes in the $\Delta^{13}C_{carb\text{-}ker}$ ($\Delta^{13}C_{carb\text{-}ker} = \delta^{13}C_{carb} - \delta^{13}C_{ker}$) help to determine periods of high and low productivity. During photosynthesis, ^{12}C is preferentially incorporated into the biomass, causing a relative ^{13}C-enrichment of the DIC reservoir in the surface waters (e.g., Hollander et al., 1993). Thus, during high productivity periods, the $\delta^{13}C$ composition of organic matter increases more than that of carbonate by 3‰ (Hollander and McKenzie, 1991). The opposite is true for low productivity periods, which lead to a buildup of CO_2 in the water column, increasing the photosynthetic isotopic fractionation. Therefore, the $\Delta^{13}C_{carb\text{-}ker}$ increase by up to 3.9‰ in the lowermost (+0.1 to +0.7 m) Scythian sediments indicates a decrease of pCO_2, caused by high productivity in the photic zone (Fig. 10). The lower C_{org}, lower ^{13}C of carbonate and organic C in the uppermost Scythian samples point to lower productivity in the water column. The laminations indicate the absence of burrowing organisms, which suggests low dissolved-O_2 content at the water–sediment interface.

The biomarkers distribution and the stable C isotope data suggest a stratified basin at Idrijca with fluctuations between anoxic and oxic conditions combined with periodic marine and probably freshwater incursions. Furthermore, for similar primary productivity rates and DIC speciation the variations in the $\delta^{13}C$ of primary

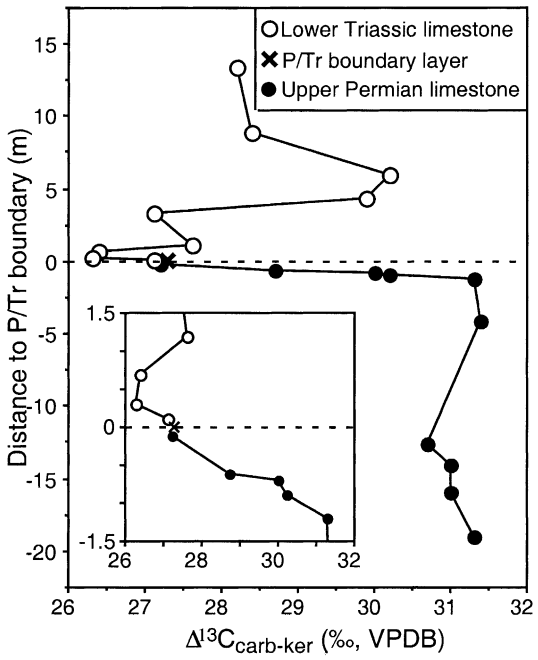

Fig. 10. Scatterplots of $\delta^{13}C_{ker}$ vs. $\delta^{13}C_{carb}$ in samples from the P/Tr section at Idrijca Valley.

organic matter may reflect (global) changes in the atmospheric CO_2 content (Popp et al., 1989; Hollander and McKenzie, 1991; Freeman and Hayes, 1992). High atmospheric CO_2 content and/or high dissolved CO_2 in cold waters cause production of ^{13}C-depleted marine plankton (e.g., Popp et al., 1989). This explains the lower $\delta^{13}C$ values in the earliest Scythian organic matter in British Columbia, Canada (−29 and −32‰, Wang et al., 1994) compared to the measured values in the Idrijca section (−26 and −28‰). Lower Canadian $\delta^{13}C$ values (3‰ on average) may be consistent with the generation of organic matter in a cool, high-latitude environment (e.g., Rau et al., 1989), whereas at the time of the P/Tr transition the Idrijca section was located within 10° of the equator (Fig. 1), and photosynthesis operated in CO_2-poor warm waters.

6. Conclusion

The organic matter in the sediments from the undisturbed and nonmetamorphosed Permian–Triassic section in the Idrijca Valley, Western Slovenia, has different sources and varying geochemical and isotopic compositions. The geochemical data and sedimentological observations indicate that sedimentation occurred in a stratified water column, with episodic variations of the vertical extension of the photic zone and primary productivity. Comparison of the alkanes distribution,

the occurrence of biomarkers and the $\delta^{13}C$ values of alkanes, pristane and phytane indicate lipid contributions from algae and bacteria throughout the Upper Permian to Lower Triassic depositions. Decrease in the C_{carb} and C_{org} contents and $\delta^{13}C$ values of carbonates, and increase of the OI indicate a decrease of the anoxia in the uppermost Permian to lowermost Scythian water column. The organic geochemical and C isotopic data record more oxygenated conditions in the uppermost Permian to lowermost Scythian marked by the occurrence of oolitic limestones. It appears that the oxygenation level of the sediments and bottom waters changed during the deposition of the P/Tr section, and strongly influenced the preservation of organic matter. ^{13}C enrichment of the kerogens of the lowermost Scythian sediments is thought to result from greater algal productivity, which occurred during the earliest Triassic transgression events. A minor input of ^{13}C-enriched terrestrial organic matter cannot be excluded. The substantial contribution of freshwater algae to the Permian–Triassic sediments is in line with the paleogeographic reconstruction of this part of the western Tethys that suggests sedimentation across the P/Tr boundary occurred in an epicontinental sea.

Acknowledgements

We thank Tadej Dolenec from the Department of Geology of the University of Ljubljana, for sharing the Idrija Valley section samples. This study benefited from financial support of the Swiss National Science Foundation (FNS grant 21-59198.99) and the University of Lausanne. Comments by B.R.T. Simoneit and constructive reviews by 3 *Applied Geochemistry* reviewers helped to improve an earlier draft of the paper. This is a contribution to IGCP 429 "Organic matter in major environmental issues".

References

Anderson, T.F., Arthur, M.A., 1983. Stable isotopes of oxygen and carbon and their application to sedimentologic and paleoenvironmental problems. In: Arthur, M.A. (Ed.), Stable Isotopes in Sedimentary Geology. Society Econ. Paleontol. Mineral., Short Course Vol. 10, pp. 1–1-15.

Arthur, A.A., Dean, W.E., Claypool, G.E., 1985. Anomalous ^{13}C enrichment in modern marine organic carbon. Nature 315, 216–218.

Baud, A., Margaritz, M., Holser, W.T., 1989. Permian–Triassic of the Tethys: carbon isotope studies. Geol. Rund 78, 649–677.

Becker, L., Poreda, R.J., Hunt, A.G., Bunch, T.E., Rampino, M., 2001. Impact event at the Permian–Triassic boundary: evidence from extraterrestrial noble gases in fullerenes. Science 291, 1530–1533.

Bowring, S.A., Erwin, D.H., Jin, Y.G., Martin, M.W., Davidek, K., Wang, W., 1998. U/Pb zircon geochronology and tempo of the end-Permian mass extinction. Science 280, 1039–1045.

Campbell, I.H., Czamanske, G.K., Fedorenko, V.A., Hill, R.L., Stepanov, V., 1992. Synchronism of the Siberian Traps and the Permian-Triassic boundary. Science 258, 1760–1763.

Czochanska, Z., Gilbert, T.D., Philp, R.P., Sheppard, C.M., Weton, R.J., Wood, T.A., Woolhouse, A.D., 1988. Geochemical application of sterane and triterpane biomarkers to a description of oils from the Taranaki Basin in New Zealand. Org. Geochem 12, 123–135.

Didyk, B.M., Simoneit, B.R.T., Brassell, S.C., Eglinton, G., 1978. Organic geochemical indicators of paleoenvironmental conditions of sedimentation. Nature 272, 216–222.

Dolenec, T., Buser, S., Dolenec, M., 1999. The Permian-Triassic boundary in the Karavanke Mountains (Slovenia): stable isotope variations in the boundary carbonate rocks of the Košutnik Creek and Brsnina section. Geologija 41, 17–27.

Dolenec, T., Lojen, S., Ramovš, A., 2001. The Permian-Triassic boundary in Western Slovenia (Idrijca Valley section): magnetostratigraphy, stable isotopes and elemental variations. Chem. Geol 175, 175–190.

Eglinton, G., Hamilton, R.J., 1963. The distribution of the *n*-alkanes. In: Swain, T. (Ed.), Chemical Plant Taxonomy. Academic Press, London, pp. 187–217.

Engel, M.H., Macko, S.A., Leythaeuser, D., 1991. The potential application of stable isotopes for distinguishing indigenous versus migrated hydrocarbons in a mature shale/sandstone sequence. Chem. Geol 93, 47–59.

Erwin, D.H., 1994. The Permo-Triassic extinction. Nature 367, 231–236.

Erwin, D.H., 1996. Permian global bio-events. In: Wallister, O. (Ed.), Global Events and Event Stratigraphy in the Phanerozoic. Springer-Verlag, Berlin, pp. 251–264.

Fogel, M.L., Cifuentes, L.A., 1993. Isotope fractionation during primary production. In: Engel, M.H., Macko, S.A. (Eds.), Org. Geochem., Principles and Applications. Plenum Press, New York, pp. 73–98.

Fowler, M.G., Abolins, P., Douglas, A.G., 1986. Monocyclic alkanes in Ordovician organic matter. Org. Geochem 10, 815–823.

Freeman, K.H., Hayes, J.M., Trendel, J.M., Albrecht, P., 1990. Evidence from carbon isotope measurements for diverse origins of sedimentary hydrocarbons. Nature 343, 254–256.

Freeman, K.H., Hayes, J.M., 1992. Fractionation of carbon isotopes by phytoplankton and estimates of ancient pCO_2 levels. Global Biogeochem. Cycles 6, 185–198.

Freeman, K.H., Wakeham, S.G., Hayes, J.M., 1994. Predictive isotopic biogeochemistry: hydrocarbons from anoxic marine basins. Org. Geochem 21, 629–644.

Galimov, E.M., 1985. The Biological Fractionation of Isotopes. Academic Press, Orlando.

Grice, K., Schouten, S., Nissenbaum, A., Charrach, J., Sinninghe Damsté, J.S., 1998. A remarkable paradox: sulfurised freshwater (*Botryococcus braunii*) lipids in an ancient hypersaline euxinic ecosystem. Org. Geochem. 28, 195–216.

Grimalt, J., Albaigés, J., 1987. Sources and occurrences of C_{12}-C_{22} *n*-alkane distributions with even carbon-number preference in sedimentary environments. Geochim. Cosmochim. Acta 51, 1379–1384.

Guthrie, J.M., 1996. Molecular and carbon isotopic analysis of individual biological markers evidence for sources of organic matter and paleoenvironmental conditions in the Upper Ordovician Maquoketa Group. Illinois Basin, U.S.A. Org. Geochem. 25, 439–460.

ten Haven, H.L., de Leeuw, J.W., Rullkötter, J., Sinningthe Damsté, J.S., 1987. Restricted utility of the pristane/phytane ratio as a palaeoenvironmental indicator. Nature 330, 641–642.

Hayes, J.M., Freeman, K.H., Popp, N., Hoham, C.H., 1990. Compound-specific isotope analysis, a novel tool for reconstruction of ancient biochemical processes. Org. Geochem 16, 1115–1128.

Hoffmann, C.F., Foster, C.B., Powell, T.G., Summons, R.E., 1987. Hydrocarbon biomarkers from Ordovician sediments and the fossil alga Gloeocapsmorpha prisca Zalessky 1917. Geochim. Cosmochim. Acta 51, 2681–2697.

Höld, I., Schouten, S., van Kaam-Peters, H.M.E., Sinninghe Damsté, J.S., 1998. Recognition of *n*-alkyl and isoprenoids algaenans in marine sediments by stable carbon isotopic analysis of pyrolysis products of kerogens. Org. Geochem. 28, 179–184.

Hollander, D.J., McKenzie, J.A., Hsü, K.J., 1993. Carbon isotope evidence for unusual plankton blooms and fluctuations of surface water CO_2 in "Strangelove Ocean" after terminal Cretaceous event. Palaeogeog., Palaeoclimatol., Palaeoecol 104, 229–237.

Hollander, D.J., McKenzie, J.A., 1991. CO_2 controls on carbon isotope fractionation during aqueous photosynthesis: a paleo-pCO_2 barometer. Geol 19, 929–932.

Hotinski, R.M., Bice, K.L., Kump, L.R., Najjar, R.G., Arthur, M.A., 2001. Ocean stagnation and end-Permian anoxia. Geol 29, 7–10.

Hunt, J.M., 1996. Petroleum Geochemistry and Geology. W.H. Freeman and Company, New York.

Jin, Y.G., Wang, Y., Wang, W., Shang, Q.H., Cao, C.Q., Erwin, D.H., 2000. Pattern of marine mass extinction near the Permian-Triassic boundary in South China. Science 289, 432–436.

Knoll, A.H., Bambach, R.T., Canfield, D.E., Grotzinger, J.P., 1996. Comparative Earth history and Late Permian mass extinction. Science 273, 452–457.

Magaritz, M., Krishnamurthy, R.V., Holser, W.T., 1992. Parallel trends in organic and inorganic carbon isotopes across the Permian/Triassic boundary. Am. J. Sci. 292, 727–739.

Meinschein, W.G., 1969. Hydrocarbons-saturated, unsaturated and aromatic. In: Eglinton, G., Murphy, M.T.J. (Eds.), Org. Geochem., Methods and Results. Springer-Verlas, Berlin, pp. 330–354.

Metzger, P., Casadewall, E., 1991. Ether lipids from *Botryococcus braunii* and their biosynthesis. Phytochem. 31, 2341–2349.

Metzger, P., Aumelas, A., 1997. Lycopanerols A, ditetraterpenoid tetraether derivatives from green microalga *Botryococcus braunii*. Tetrahed. Lett. 28, 3931–3934.

McCrea, J.M., 1950. The isotopic chemistry of carbonates and a paleotemperature scale. J. Chem. Phy 18, 849–857.

Palmer, S.E., 1993. Effect of biodegradation and water washing on crude oil composition. In: Engel, M.H., Macko, S.A. (Eds.), Org. Geochem., Principles and Applications. Plenum Press, New York, pp. 511–533.

Peters, K.E., 1986. Guidelines for evaluating petroleum source rock using programmed pyrolysis. Am. Assoc. Petrol. Geol. Bull 70, 318–329.

Peters, K.E., Moldowan, J.M., 1993. The Biomarker Guide. Interpreting Molecular Fossils in Petroleum and Ancient Sediments. Prentice Hall, Englewood Cliffs.

Philp, R.P., 1980. Comparative organic geochemical studies of recent algal mats and sediments of algal origin. In: Trudinger, P.A., Walter, M.R., Ralph, B.J. (Eds.), Biogeochemistry of Ancient and Modern Environments. Springer-Verlag, Berlin, pp. 173–187.

Popp, B.N., Takigiku, R., Hayes, J.M., Louda, J.W., Baker, E.W., 1989. The post-Paleozoic chronology and mechanism of ^{13}C depletion in primary marine organic matter. Am. J. S 289, 436–454.

Ramovš, A., 1986. Marine development of the uppermost Žažar beds and the lowermost Scythian beds. Permian and Permian-Triassic boundary in the South Alpine segment of the Western Tethys. IGCP Project 203, Excursion Guidebook 39–42.

Rampino, M.R., Haggerty, B.M., 1996. Hazards Due to Asteroids. University of Arizona Press, Tucson.

Rampino, M.E., Prokoph, A., Adler, A., 2000. Tempo of the end-Permian event: high-resolution cyclostratigraphy at the Permian-Triassic boundary. Geology 7, 643–646.

Rau, G.H., Takahashi, T., Des Marais, D.J., 1989. Latitudinal variations in plankton $\delta^{13}C$: implications for CO_2 and productivity in past oceans. Nature 341, 516–528.

Raup, D.M., 1979. Size of the Permian-Triassic bottleneck and its evolutionary implications. Science 206, 217–218.

Renne, P.R., Zichao, Z., Richards, M.A., Black, M.T., Basu, A.R., 1995. Synchronology and causal relations between Permian-Triassic boundary crises and Siberian flood volcanism. Science 269, 1413–1416.

Retallack, G.J., 1999. Postapocalyptic greenhouse paleoclimate revealed by earliest Triassic Paleodsols in the Sydney Basin, Australia. Geol. Soc. Am. Bull 111, 52–70.

Rubinstein, I., Strausz, O.P., 1979. Geochemistry of the thiourea adduct fraction from an Alberta petroleum. Geochim. Cosmochim. Acta 43, 1387–1392.

Schidlowski, M., 1982. Content and isotopic composition of reduced carbon in sediments. In: Holland, H.D. (Ed.), Earth's Earliest Biosphere: Its Origin and Evolution. Princeton University Press, Princeton, pp. 149–186.

Schulze, T., Michaelis, W., 1990. Structure and origin of terpenoid hydrocarbons in some German coals. Org. Geochem 16, 1051–1058.

Spangenberg, J.E., Macko, S.A., 1998. Organic geochemistry of the San Vicente zinc-lead district, eastern Pucará Basin, Peru. Chem. Geol 146, 1–23.

Stahl, W.J., 1978. Source rock-crude oil correlation by isotopic type-curves. Geochim. Cosmochim. Acta 42, 1573–1577.

Stampfli, G., Borel, G., Mosar, J., Ziegler, P.A., 2001. The Paleotectonic Atlas of the Peritethyan Domain. CD-R. European Geophysical Society.

Stanley, S.M., Yang, X., 1994. A double mass extinction at the end of the Paleozoic Era. Science 266, 1340–1344.

Sukh Dev, 1989. Terpenoids. In: Rowe, J.W. (Ed.), Natural Products of Woody Plants I. Springer-Verlag, Berlin, pp. 691–807.

Thackeray, J.F., van der Merwe, N.J., Lee-Thorp, J.A., Sillen, A., Lanham, J.J., Smith, R., Keyser, A., Monteiro, P.M.E.,

1990. Carbon isotopic evidence from late Permian Therapsids teeth, for a progressive change in atmospheric CO_2 composition. Nature 347, 751–753.

Tissot, B.P., Welte, D.H., 1984. Petroleum Formation and Occurrence. Springer-Verlag, Berlin.

Veizer, J., 1983. Trace elements and isotopes in sedimentary carbonates. Review in Mineralogy 11, 265–299.

Wang, K., Geldsetzer, H.H.J., Krouse, H.R., 1994. Permian-Triassic extinction: organic $\delta^{13}C$ evidence from British Columbia, Canada. Geol. 22, 580–584.

Waples, D., Haug, P., Welte, D.H., 1974. Occurrence of the regular C_{25} isoprenoid hydrocarbon in Tertiary sediments representing a lagoon-type saline environment. Geochim. Cosmochim. Acta 8, 381–387.

Whelan, J.K., Thompson-Rizer, C.L., 1993. Chemical methods for assessing kerogen and protokerogen types and maturity. In: Engel, M.H., Macko, S.A. (Eds.), Org. Geochem., Principles and Applications. Plenum Press, New York, pp. 289–353.

Wignall, P.B., Hallam, A., 1992. Anoxia as a cause of the Permian/Triassic mass extinction: facies evidence from northern Italy and the western United States. Palaeogeog., Palaeoclimatol., Palaeoecol 93, 21–46.

Wignall, P.B., Twitchett, R.J., 1996. Oceanic anoxia and the end Permian mass extinction. Science 272, 1155–1158.

Wolf, M., David, P., Eckardt, C.B., Hagemann, H.W., Püttmann, W., 1989. Facies and rank of the Permian Kupferschiefer from the lower Rhine Basin and NW Germany. Internat. J. Coal Geol 14, 119–136.